

Iridium-catalysed 3,5-bis-borylation of phthalonitrile enables access to a family of C_{4h} octaarylphthalocyanines

Electronic Supporting Information

Katie D. Mulholland,^a Sangbin Yoon,^a Christopher C. Rennie,^b Eleanor K. Sitch,^a
Alasdair I. McKay,^c Katharina Edkins,^d and Robert M. Edkins^{b*}

^a Chemistry Research Laboratory, University of Oxford, 12 Mansfield Road, Oxford
OX1 3TA, United Kingdom.

^b WestCHEM Department of Pure and Applied Chemistry, Thomas Graham Building,
University of Strathclyde, 295 Cathedral Street, Glasgow G1 1XL, United Kingdom.

^c School of Chemistry, Monash University, Clayton, VIC 3800, Australia.

^d Division of Pharmacy and Optometry, University of Manchester, Stopford Building,
Manchester M13 9PT, United Kingdom.

Email: robert.edkins@strath.ac.uk

Contents

Experimental Section	S3-S5
General Information	S3
Single-Crystal X-ray Diffraction	S3
General Photophysical Measurements	S4-S5
Synthesis	S6-S11
4-(Bpin)phthalonitrile, 1 , and 3,5-bis(Bpin)phthalonitrile, 2	S6
Improved synthesis of 3,5-bis(Bpin)phthalonitrile, 2	S7
3,5-Bis-(3',5'-bis(trifluoromethyl)phenyl)-1,2-dicyanobenzene, 3	S7
3,5-Bis-(3',5'-bis(tert-butyl)phenyl)-1,2-dicyanobenzene, 4	S7-S8
3,5-Bis-(3',5'-bis(methoxy)phenyl)-1,2-dicyanobenzene, 5	S8
ZnPc(Ar ^{CF3}) ₈ , 6	S9
ZnPc(Ar ^{tBu}) ₈ , 7	S9
ZnPc(Ar ^{OMe}) ₈ , 8	S10
MgPc(Ar ^{CF3}) ₈ , 9	S10
H ₂ Pc(Ar ^{CF3}) ₈ , 10	S11
NMR Spectra	S12-S22
¹ H, ¹¹ B{ ¹ H} and ¹³ C{ ¹ H} NMR spectra of 1	S12-S13
¹ H, ¹¹ B{ ¹ H} and ¹³ C{ ¹ H} NMR spectra of 2	S13-S14
¹ H, ¹⁹ F and ¹³ C{ ¹ H} NMR spectra of 3	S15-S16
¹ H and ¹³ C{ ¹ H} NMR spectra of 4	S16-S17
¹ H and ¹³ C{ ¹ H} NMR spectra of 5	S17-S18
¹ H and ¹⁹ F NMR spectra of 6	S18-S19
¹ H NMR spectrum of 7	S19
¹ H NMR spectrum of 8	S20
¹ H and ¹⁹ F NMR spectra of 9	S20-S21
¹ H and ¹⁹ F NMR spectra of 10	S21-S22
Single-Crystal X-ray Diffraction (SC-XRD) Data	S23-24
Molecular structures of 1-5 from SC-XRD	S25
Molecular structure of 7 from SC-XRD	S25
Absorption and Emission Spectra	S26-S29
Comparison of absorption spectra of 6 , 9 , and 10	S26
Concentration-dependent absorption spectra of 9	S26
Solvent-dependent absorption spectra of 6	S27
Solvent-dependent emission spectra of 6	S27
Solvent-dependent absorption spectra of 7	S28
Solvent-dependent emission spectra of 7	S28
Solvent-dependent absorption spectra of 8	S29
Solvent-dependent emission spectra of 8	S29
References	S30

Experimental Section

General Information. Reactions were performed in oven-dried glassware using standard Schlenk techniques under a dry nitrogen or argon atmosphere. Solvents used for reactions were HPLC grade. Methyl *tert*-butyl ether (MTBE) was dried over activated 4-Å molecular sieves. $[\text{Ir}(\text{COD})(\mu\text{-OMe})]_2$ (COD = 1,5-cyclooctadiene) was synthesized according to the literature.¹ All other starting materials were purchased from commercial sources and were used without further purification, except for B_2pin_2 , which was a gift from AllyChem Co., Ltd. (Dalian, China).

Thin layer chromatography (TLC) was performed on aluminium-backed plates pre-coated with a layer of silica and fluorescent indicator (Polygram Sil G/UV₂₅₄) from Marchery-Nagel. Column chromatography was performed using Silica Gel 60 (40-63 microns). Solvents were removed *in vacuo* using a rotary evaporator at a maximum temperature of 40 °C.

Solution NMR spectroscopic data were obtained at room temperature (r.t.) in aerated, deuterated solvents using the following models of Bruker spectrometer: AVIII 400, AVIII HD 400, AVIII 500, AVIII HD 500, and AVII 500. All chemical shifts (δ) were referenced to solvent peaks as follows: ^1H NMR spectra were referenced to residual protiated solvent; $^{13}\text{C}\{^1\text{H}\}$ spectra were referenced to benzene- d_6 (128.06 ppm), CDCl_3 (77.16 ppm), CD_2Cl_2 (54.00 ppm), or acetone- d_6 (29.84 ppm); $^{19}\text{F}\{^1\text{H}\}$ NMR signals were referenced to CFCl_3 *via* the deuterium lock; and $^{11}\text{B}\{^1\text{H}\}$ NMR signals were referenced to $\text{BF}_3\cdot\text{OEt}_2$ *via* the deuterium lock. Electrospray ionization (ESI) mass spectrometry (MS) was performed on a Waters LCT Premier XE and MALDI MS on a Micromass m@lDi MS Micro using Masslinks 4.1 software.

Single-Crystal X-ray Diffraction. Crystals were soaked in perfluoro polyether oil, mounted onto MiTeGen sample holders and placed directly into a pre-cooled cryostream. Crystals of **5** were measured on an Oxford Diffraction Excalibur (Rigaku) using Mo-K_α radiation (0.71073 Å). Crystals of **9** were measured on an Oxford Diffraction/Agilent SuperNova A diffractometer using Cu-K_α radiation (1.54178 Å). The data were processed using CrysAlis 38.46 software. All other structures were measured on a Bruker (Karlsruhe, Germany) D8 Quest diffractometer using Mo-K_α radiation (0.71073 Å) or Cu-K_α radiation (1.54178 Å). The data were processed using Bruker Apex-III software. All structures were solved in Olex2² using Olex.solve and

refined using ShelXL. All non-H atoms were located from Fourier difference maps and refined anisotropically. H atoms were calculated as geometrical riding models on the heavy atom and refined isotropically. Heavily disordered solvent was masked for the final refinement using the OLEX2 solvent mask for the structures of **3**, **7**, and **9**.

All pictures of molecular structures have been generated in OLEX2 (ver. 1.2). General color code: hydrogen (white), boron (yellow), carbon (white), nitrogen (blue), oxygen (red), fluorine (green), zinc (dark blue), magnesium (cyan). Atomic displacement ellipsoids are drawn at 50%, except where a ball and stick model has been used for clarity (**6**, **7**, and **9**, which diffracted poorly due to being thin plates as well as containing significant disorder and/or solvent, but nonetheless unequivocally confirm the molecular symmetry of the Pcs as C_{4h}). Crystal data and experimental details are listed in Table S1. Full structural information has been deposited with Cambridge Structural Database, CCDC 1989433-1989438 and 1989726-1989727.

General Photophysical Measurements. All measurements were performed in standard quartz cuvettes with path lengths of 1, 5, or 10 mm. UV-visible absorption spectra were recorded using either a PG Instruments T60U or an Agilent Cary 60 spectrophotometer. The molar extinction coefficients were calculated from three independently prepared samples in acetone solution.

The emission spectra were recorded using a Horiba Jobin-Yvon Fluorolog 3-12 spectrometer equipped with a double monochromator for emission, operating in right-angle geometry mode, and all spectra were fully corrected for the spectral response of the instrument. All solutions used in fluorescence measurements had a concentration lower than 5×10^{-6} M to minimize inner filter effects, unless stated otherwise.

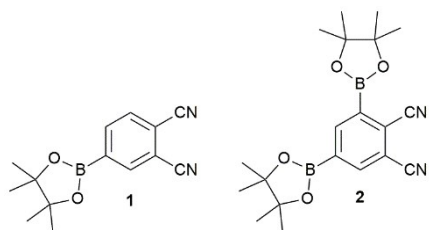
Fluorescence lifetimes were recorded using the time-correlated single-photon counting (TCSPC) method using the double emission monochromator and Hamamatsu R928 PMT installed on the Fluorolog 3-12 spectrometer and an Edinburgh Instruments TCSPC card. Solutions were excited with a pulsed diode laser at a wavelength of 374 nm at repetition rates of 20 MHz. The full-width-at-half-maximum (FWHM) of the pulse from the diode laser was *ca.* 60 ps with an instrument response function (IRF) of *ca.* 600 ps FWHM. The IRFs were measured from the scatter of an aqueous suspension of Ludox at the excitation wavelength. Decays were recorded to 10 000 counts in the peak channel with a record length of 2048

channels. The band pass of the emission monochromator was adjusted to give a signal count rate of <100 kHz. Iterative reconvolution of the IRF with one exponential decay function and non-linear least-squares analysis were used to analyse the data. The quality of all decay fits was judged to be satisfactory, based on the calculated values of the reduced χ^2 and Durbin-Watson parameters and visual inspection of the weighted residuals.

Fluorescence quantum yields were measured by the relative method using zinc phthalocyanine ($\Phi_f = 0.17$ in acetone) as a suitable standard.³ The singlet-oxygen quantum yield of **6** in DMSO solution was measured using a procedure adapted from the literature.⁴ Briefly, the relative rate of decomposition of 1,3-diphenylisobenzofuran (DPBF) upon reaction with singlet oxygen generated by irradiating DMSO solutions of **6** at 706 nm and reference compound zinc phthalocyanine (ZnPc) at 670 nm in stirred 1-cm path length cuvettes was monitored by UV-visible absorption spectroscopy. A 3.0×10^{-5} M DPBF DMSO solution was used to make solutions of **6** and ZnPc with an optical density of 0.2 at the maximum of the Q band of the respective phthalocyanine. The Xe lamp of the Jobin-Yvon Horiba Fluorolog-3 fluorimeter was used to irradiate the sample using a band pass of 5 nm. The absorption spectrum of the DPBF solution was recorded at time intervals of 1 minute using the PG Instruments T60U spectrophotometer and a graph of change in absorbance at the absorption maximum of DPBF over time was plotted. The final quantum yield value was corrected for the wavelength dependence and temporal fluctuations of the lamp by multiplying the calculated value by the ratio of the time-averaged corrected reference photodiode signals of the spectrometer measured during excitation.

Synthesis

4-(Bpin)phthalonitrile, **1**, and 3,5-bis(Bpin)phthalonitrile, **2**



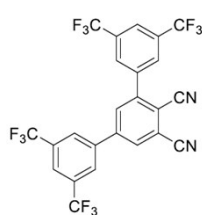
[Ir(COD)(OMe)]₂ (396 mg, 1.5 mol%) and 4,4'-bis(*tert*-butyl)-2,2'-bipyridyl (dtbpy) (320 mg, 3 mol%) were added to dry, degassed MTBE (40 mL). A portion of B₂pin₂ (pin = pinacolato) (*ca.* 3.20 g of 11.16 g total, 44 mmol) was added and the mixture stirred for a few minutes. 1,2-Dicyanobenzene (5.12 g, 40 mmol) and the remaining B₂pin₂ were added. The solution was then heated at reflux (55 °C) for 24 h. The mixture was cooled to r.t. and filtered through a silica pad eluting with 1:1 CH₂Cl₂:hexane. The filtrate was collected until a yellow band had eluted. The solvent was removed under reduced pressure, affording a brown solid. The residual crude solid was ground to a fine powder and heated at 50 °C/0.3 mbar in a sublimation apparatus, causing sublimation of a small amount of unreacted phthalonitrile, which was discarded. Once phthalonitrile sublimation ceased, the mixture was heated at 158 °C/0.3 mbar for 5 h. **1** condensed on the cold finger as a white solid. (1.7 g, 17%, 98% pure by ¹H NMR with *ca.* 2% **2** as impurity). ¹H NMR (CDCl₃, 400 MHz) δ_H (ppm): 8.18 (1 H, s), 8.10 (1 H, d, ³J_{HH} = 7.8 Hz), 7.78 (1 H, d, ³J_{HH} = 7.8 Hz), 1.34 (12 H, s). ¹¹B{¹H} NMR (CDCl₃, 128 MHz) δ_B (ppm): 29.8 (s, br.). ¹³C{¹H} NMR (CDCl₃, 101 MHz) δ_C (ppm): 139.4, 138.9, 132.6, 117.5, 115.5 (2 C resolved), 115.2, 85.3, 24.9. Peak for C–Bpin not conclusively observed due to quadrupolar broadening. ESI⁺ (MeOH): *m/z* = 277.0 ([M+Na]⁺).

The brown solid remaining after the sublimation was recrystallized by slowly cooling a saturated MTBE solution of the crude material from 55 °C to r.t.. The obtained crystals were washed with cold (–15 °C) MTBE, affording **2** as a white crystalline solid. The procedure was repeated on the residue recovered from the solution separated from the first recrystallization to afford a second crop of white solid (3.6 g in total, 24%). ¹H NMR (CDCl₃, 500 MHz) δ_H (ppm): 8.48 (1 H, s), 8.26 (1 H, s), 1.41 (12 H, s), 1.38 (12 H, s). ¹¹B{¹H} NMR (CDCl₃, 160 MHz) δ_B (ppm): 30.0 (s, br.). ¹³C{¹H} NMR (CDCl₃, 126 MHz) δ_C (ppm): 145.2, 141.2, 122.3, 116.5, 116.0, 115.5, 85.6, 85.3, 25.0, 24.9. Peaks for C–Bpin not conclusively observed due to quadrupolar broadening. ESI⁺ (MeOH): *m/z* = 381.2 ([M+H]⁺).

Improved synthesis of 3,5-bis(Bpin)phthalonitrile, **2**

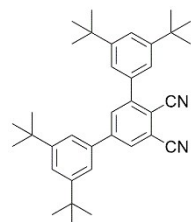
[Ir(COD)(OMe)]₂ (195 mg, 1.5 mol%) and dtbpy (157 mg, 3 mol%) were added to dry, degassed MTBE (15 mL). B₂pin₂ (7.43 g, 29.3 mmol) was added portionwise and the mixture stirred for a few minutes. 1,2-Dicyanobenzene (2.50 g, 19.5 mmol) was added and the solution was heated at reflux (55 °C) for 24 h at which point the reaction mixture had solidified. The crude solid was recrystallized from hot MTBE to afford **2** as a white powder (3.43 g, 46%). Analyses matched those reported above.

3,5-Bis-(3',5'-bis(trifluoromethyl)phenyl)-1,2-dicyanobenzene, **3**



Compound **2** (500 mg, 1.32 mmol) was dissolved in 1,4-dioxane (15 mL). 3,5-Bis(trifluoromethyl)-1-iodobenzene (0.94 mL, 1.80 g, 5.30 mmol) and CsCO₃ (1.72 g, 5.28 mmol) were added and the solution was degassed by three vacuum/N₂ cycles. Pd₂(dba)₃ (60 mg, 5 mol%) and SPhos (108 mg, 20 mol%) were added and the reaction mixture was heated at 65 °C for 24 h. The mixture was cooled to r.t., diluted with EtOAc, and washed with brine. The organic layer was separated, dried over MgSO₄, and concentrated under reduced pressure. The resulting oil was dissolved in a minimum amount of CH₂Cl₂, layered with hexane and left to crystallize for 48 h. Residual solvent was removed by pipette, leaving **3** as white crystals (497 mg, 68%). ¹H NMR (acetone-d₆, 400 MHz) δ_H (ppm): 8.80 (1 H, s), 8.79 (1 H, s), 8.66 (2 H, s), 8.52 (2 H, s), 8.29 (1 H, s), 8.22 (1 H, s). ¹⁹F{¹H} NMR (acetone-d₆, 470 MHz) δ_F (ppm): -63.26 (1 F, s), -63.30 (1 F, s). ¹³C{¹H} NMR (acetone-d₆, 126 MHz) δ_C (ppm): 145.2, 143.9, 140.5, 140.1, 134.7, 133.6, 133.1 (q, ²J_{CF} = 33 Hz, C-CF₃), 132.6 (q, ²J_{CF} = 33 Hz, C-CF₃), 131.1 (m), 129.5 (m), 124.3 (q, ¹J_{CF} = 274 Hz, CF₃), 124.2 (q, ¹J_{CF} = 274 Hz, CF₃), 124.2 (septet, ³J_{CF} ≈ 4 Hz), 124.0 (septet, ³J_{CF} ≈ 4 Hz), 118.6, 116.3, 115.8, 115.7. ESI⁺ (MeOH): m/z = 553.0 ([M+H]⁺).

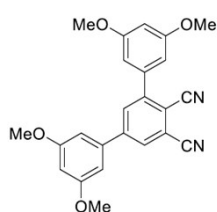
3,5-Bis-(3',5'-bis(*tert*-butyl)phenyl)-1,2-dicyanobenzene, **4**



Compound **2** (0.38 g, 1.0 mmol) was dissolved in 1,4-dioxane (10 mL). CsF (0.61 g, 4.0 mmol) and 1-bromo-3,5-di-*tert*-butylbenzene (646 mg, 2.40 mmol) were added and the solution was degassed by three vacuum/N₂ cycles. Pd₂(dba)₃ (46 mg, 5 mol%) and SPhos (82 mg, 20 mol%) were added and the reaction mixture was heated at 65 °C for 24 h. The solvent was removed under

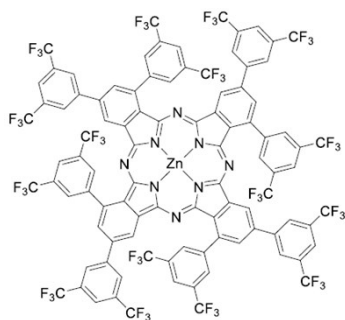
reduced pressure and the residue was suspended in EtOAc and filtered through a silica pad, eluting with EtOAc and collecting the filtrate until an orange band had eluted. The solution was concentrated under reduced pressure and the residue was purified by column chromatography on silica gel using 9:1 hexane:EtOAc as the eluent to afford **4** as a white solid. (250 mg, 50%). **¹H NMR** (CD₂Cl₂, 500 MHz) δ_{H} (ppm): 8.01 (1 H, d, $^4J_{\text{HH}} = 1.7$ Hz), 7.99 (1 H, d, $^4J_{\text{HH}} = 1.7$ Hz), 7.61 (1 H, t, $^4J_{\text{HH}} = 1.7$ Hz), 7.58 (1 H, t, $^4J_{\text{HH}} = 1.7$ Hz), 7.46 (2 H, d, $^4J_{\text{HH}} = 1.7$ Hz), 7.45 (2 H, d, $^4J_{\text{HH}} = 1.7$ Hz), 1.39 (18 H, s), 1.38 (18 H, s). **¹³C{¹H} NMR** (CD₂Cl₂, 126 MHz) δ_{C} (ppm): 152.2, 151.7, 148.6, 147.3, 136.9, 136.2, 132.8, 130.7, 123.9, 123.6, 123.3, 121.7, 117.3, 116.2, 116.0, 112.4, 35.05, 34.99, 31.14, 31.10. **ESI⁺** (MeOH): $m/z = 505.4$ ([M+H]⁺).

3,5-Bis-(3',5'-bis(methoxy)phenyl)-1,2-dicyanobenzene, **5**



Compound **2** (1.0 g, 2.6 mmol) was dissolved in 1,4-dioxane (26 mL). CsF (1.6 g, 11 mmol) and 3,5-bis(methoxy)bromobenzene (1.37 g, 6.31 mmol) were added and the solution was degassed by three vacuum/N₂ cycles. Pd₂(dba)₃ (120 mg, 5 mol%) and SPhos (220 mg, 20 mol%) were added and the solution was heated at 65 °C for 24 h. The resultant viscous orange suspension was diluted with THF and filtered through a celite plug. The eluted solution was concentrated under reduced pressure and the resulting solid was dissolved in 2:1 hexane:EtOAc (40 mL) using gentle heating, before leaving to cool to room temperature. Solid precipitate formed and the remaining solvent was removed by pipette. The solid was then dissolved in a minimum amount of CHCl₃ and kept in a 5 °C fridge for a few hours, before returning to r.t. and leaving for an additional 2 h. Solid white precipitate formed and the remaining yellow solution was removed and concentrated to give **5** as a white solid (222 mg, 21%). **¹H NMR** (CDCl₃, 400 MHz) δ_{H} (ppm): 7.95 (1 H, d, $^4J_{\text{HH}} = 1.8$ Hz), 7.90 (1 H, d, $^4J_{\text{HH}} = 1.8$ Hz), 6.70 (2 H, d, $^4J_{\text{HH}} = 2.2$ Hz), 6.69 (2 H, d, $^4J_{\text{HH}} = 2.2$ Hz), 6.59 (1 H, t, $^4J_{\text{HH}} = 2.2$ Hz), 6.57 (1 H, t, $^4J_{\text{HH}} = 2.2$ Hz), 3.86 (2 × 6 H, resolved 2 × s overlapping). **¹³C{¹H} NMR** (acetone-*d*₆, 126 MHz) δ_{C} (ppm): 161.7, 161.2, 147.2, 145.8, 139.1, 138.8, 132.4, 131.0, 117.2, 115.9, 115.5, 112.6, 107.1, 105.5, 101.5, 101.1, 55.1. **ESI⁺** (MeOH): $m/z = 401.2$ ([M+H]⁺).

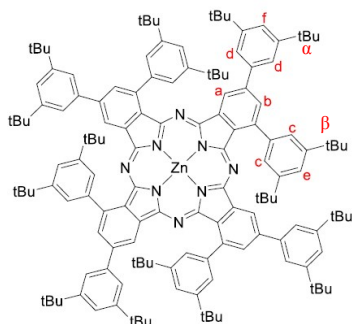
ZnPc(Ar^{CF3})₈, **6**



1,8-Diazabicycloundec-7-ene (DBU, 27 μ L, 28 mg, 0.18 mmol), Zn(OAc)₂·2H₂O (8.0 mg, 0.044 mmol) and **3** (100 mg, 0.18 mmol) in *n*-pentanol (2 mL) were heated at 132 °C for 28 h. After cooling to r.t., *n*-pentanol was removed under high vacuum. A minimal amount of acetone was used to dissolve the solid residue, and excess pyridine was added. The solution was left overnight in an

open flask to concentrate, forming a green precipitate. The green precipitate was isolated in a 0.22- μ m PTFE syringe filter, washed with CHCl₃, and recovered using acetone. The solvent was removed under reduced pressure, yielding **6** as a bright green solid (40 mg, 39% based on **3**). **¹H NMR** (acetone-*d*₆, 400 MHz) δ_{H} (ppm): 9.10 (2 H, s), 8.80 (1 H, s), 8.72 (1 H, s), 8.63 (2 H, s), 8.37 (1 H, s), 8.32 (1 H, s). **¹⁹F{¹H} NMR** (acetone-*d*₆, 377 MHz) δ_{F} (ppm): -62.82 (1 F, s), -62.98 (1 F, s). **MALDI⁺**: m/z 2274.31 ([M]⁺). **UV-visible absorption**: λ_{max} (Q band) = 695 nm ($3.8 \times 10^5 \text{ M}^{-1} \text{ cm}^{-1}$).

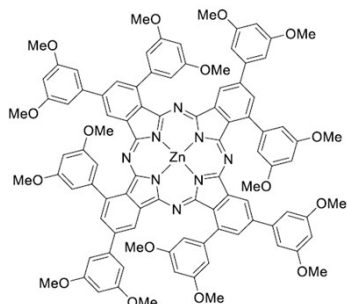
ZnPc(Ar^{tBu})₈, **7**



A solution of DBU (47 μ L, 48 mg, 0.31 mmol), Zn(OAc)₂·2H₂O (40 mg, 0.22 mmol) and **4** (100 mg, 0.20 mmol) in *n*-pentanol (1 mL) was heated at 132 °C for 16 h. After cooling to r.t., MeOH (3 mL) and water (10 mL) were added to the solution, forming a green precipitate which was isolated in a 0.22- μ m PTFE syringe filter and recovered using CH₂Cl₂. The solvent was removed

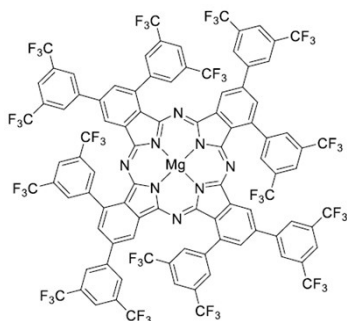
under reduced pressure. A minimal amount of acetone was used to dissolve the residual solid. The solution was kept in a 5 °C fridge overnight, and the precipitate formed was isolated, yielding product **7** as a green solid (26 mg, 25% based on **4**). **¹H NMR** (benzene-*d*₆, 500 MHz) δ_{H} (ppm): 9.19 (1 H, d, ⁴*J*_{HH} = 1.3 Hz, CH _{α}), 8.43 (1 H, d, ⁴*J*_{HH} = 1.3 Hz, CH _{β}), 8.39 (2 H, d, ⁴*J*_{HH} = 1.6 Hz, CH _{γ}), 7.76 (2 H, d, CH _{δ} , ⁴*J*_{HH} = 1.6 Hz), 7.75 (1 H, t, ⁴*J*_{HH} = 1.6 Hz, CH _{ϵ}), 7.70 (1 H, t, ⁴*J*_{HH} = 1.6 Hz, CH _{ζ}), 1.43 (18 H, s, *t*Bu- α), 1.36 (18 H, s, br., *t*Bu- β). Peaks assigned *via* a series of 1D NOESY and ¹H-¹H COSY NMR spectra. **MALDI⁺**: m/z 2083.21 ([M]⁺). **UV-visible absorption**: λ_{max} (Q band) = 704 nm.

ZnPc(Ar^{OMe})₈, **8**



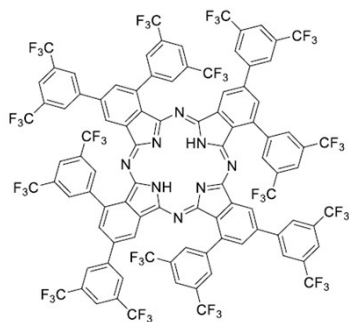
A solution of DBU (37 μ L, 38 mg, 0.25 mmol), Zn(OAc)₂·2H₂O (10 mg, 0.046 mmol) and **5** (100 g, 0.25 mmol) in *n*-pentanol (2.5 mL) were heated at 132 °C for 16 h. After cooling to r.t., MeOH (3 mL) and water (10 mL) were added to the solution, forming a green precipitate, which was isolated in a 0.22- μ m syringe filter and recovered using CH₂Cl₂. The solvent was removed under reduced pressure. The residue was purified by column chromatography (SiO₂; 50:50:1, CH₂Cl₂:toluene:pyridine). The major green band was collected, dissolved in a minimum amount of acetone, and kept in a 5 °C fridge overnight. The precipitate which formed was collected and dried, affording **8** as a green solid (14 mg, 13% based on **5**). **¹H NMR** (benzene-*d*₆, 400 MHz) δ_{H} (ppm): 9.00 (1 H, s), 8.34 (1 H, s), 7.51 (2 H, s), 7.26 (2 H, s), 7.05 (1 H, s), 6.70 (1 H, s), 4.03 (6 H, s), 3.83 (6 H, s). **MALDI⁺**: m/z 1667.49 ([M]⁺). **UV-visible absorption**: λ_{max} (Q band) = 700 nm.

MgPc(Ar^{CF3})₈, **9**



DBU (27 μ L, 28 mg, 0.18 mmol), Mg(OAc)₂·4H₂O (10.0 mg, 0.047 mmol) and **3** (100 mg, 0.18 mmol) in *n*-pentanol (1 mL) were heated at 132 °C for 28 h. After cooling to r.t., *n*-pentanol was removed under high vacuum. The green mixture was suspended in CHCl₃, isolated in a 0.22- μ m PTFE syringe filter, and recovered using acetone. The solvent was removed under reduced pressure, yielding **6** as a bright green solid (5 mg, 5% based on **3**). **¹H NMR** (acetone-*d*₆, 400 MHz) δ_{H} (ppm): 9.09 (2 H, s), 8.76 (1 H, s), 8.61 (3 H, s), 8.33 (1 H, s), 8.30 (1 H, s). **¹⁹F{¹H} NMR** (acetone-*d*₆, 377 MHz) δ_{F} (ppm): -62.83 (s), -62.99 (s). **MALDI⁺**: m/z = 2234.38 ([M]⁺). **UV-visible absorption**: λ_{max} (Q band) = 695 nm.

$\text{H}_2\text{Pc}(\text{Ar}^{\text{CF}_3})_8$, **10**



One-pot procedure: DBU (27 μL , 28 mg, 0.18 mmol), $\text{Mg}(\text{OAc})_2 \cdot 4\text{H}_2\text{O}$ (10.0 mg, 0.047 mmol) and **3** (75 mg, 0.14 mmol) in *n*-pentanol (2 mL) were heated at 132 $^\circ\text{C}$ for 16 h. After cooling to r.t., *n*-pentanol was removed under high vacuum. The green solid was then dissolved in acetone (5 mL) and HCl (1 M, 5 mL) was added. The mixture was heated at 60 $^\circ\text{C}$ and monitored by

^{19}F NMR spectroscopy until full conversion of the starting material had occurred. After 16 h the mixture was neutralized with aqueous NaHCO_3 solution and the product was extracted with CH_2Cl_2 . The product was purified by column chromatography (SiO_2 ; 1:1 hexane:EtOAc), yielding **10** as a bright green solid (4 mg, 5% based on **3**). ^1H NMR (acetone- d_6 , 400 MHz) δ_{H} (ppm): 8.49 (2 H, s), 8.39 (1 H, d, $J = 1.5$ Hz), 8.32 (2 H, s), 8.29 (1 H, d, $J = 1.5$ Hz), 8.04 (2 H, s), 0.00 (s, 2H, NH exchange with D_2O shake). $^{19}\text{F}\{^1\text{H}\}$ NMR (acetone- d_6 , 377 MHz) δ_{F} (ppm): -63.19 (s), -63.22 (s). MALDI $^+$: m/z 2211.20 $[\text{M}]^+$. UV-visible absorption: $\lambda_{\text{max}}(\text{Q}_x \text{ and } \text{Q}_y) = 688 \text{ and } 720 \text{ nm}$.

NMR Spectra

All spectra were recorded at room temperature

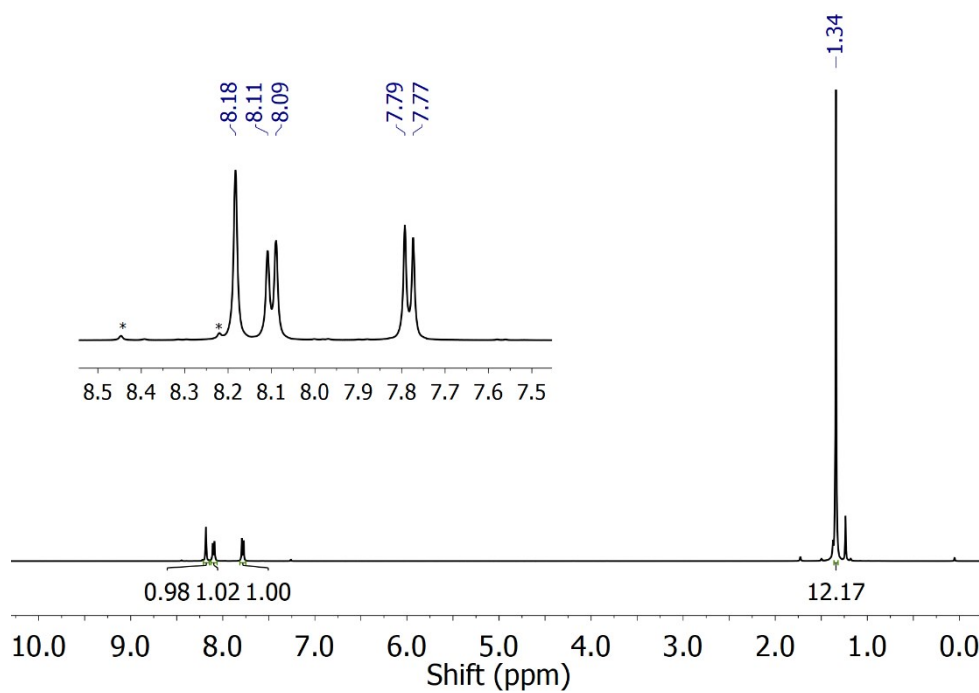


Figure S1. ¹H NMR spectrum of **1** in CDCl₃ at 400 MHz (* = residual **2**)

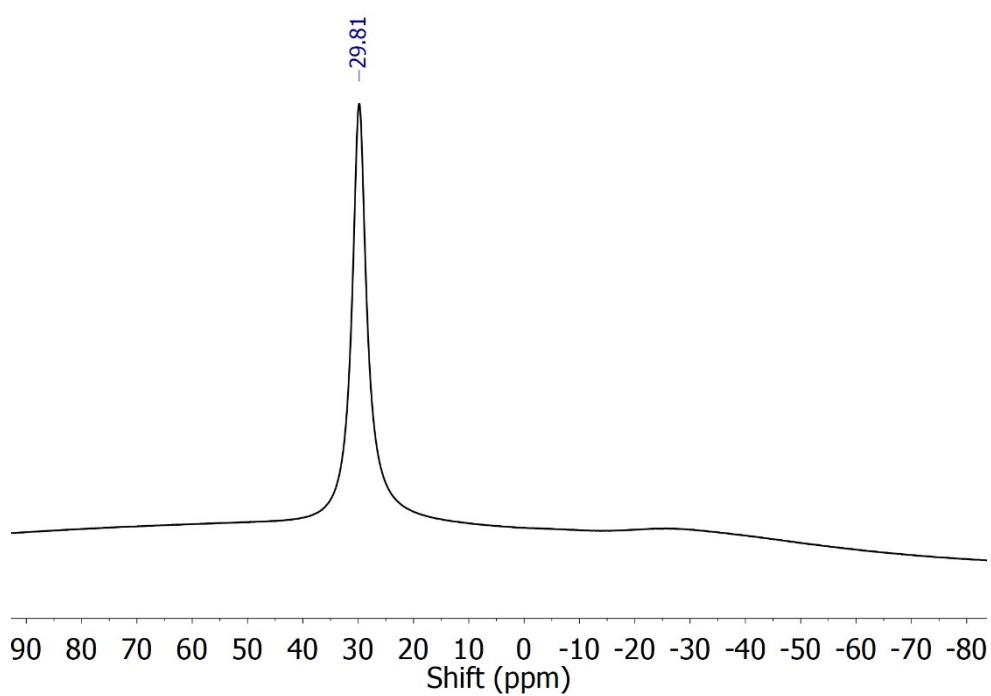


Figure S2. ¹¹B{¹H} NMR spectrum of **1** in CDCl₃ at 128 MHz

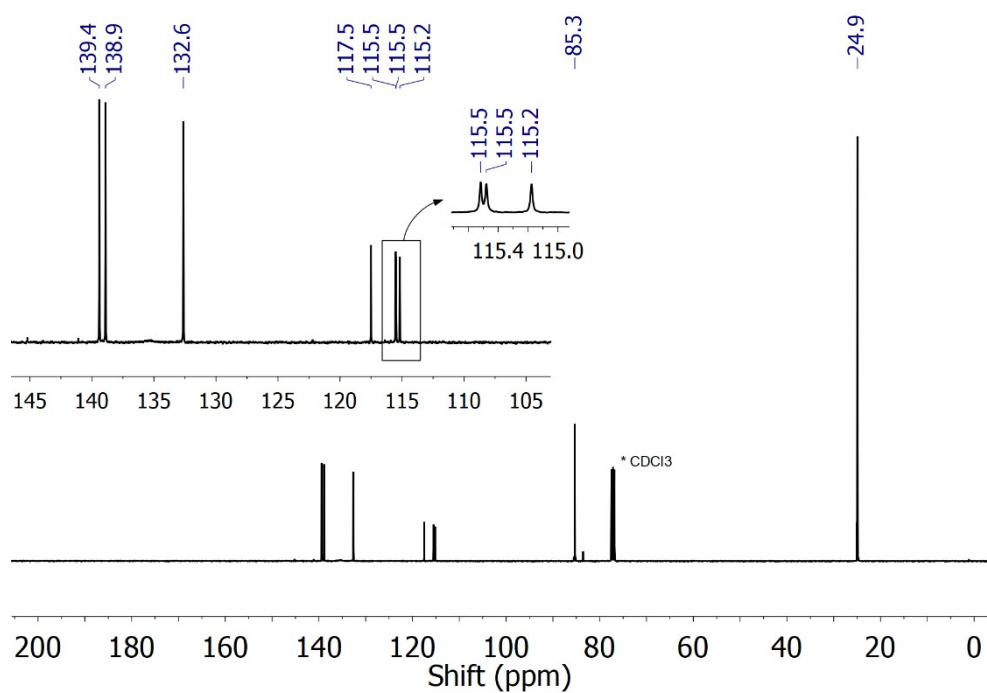


Figure S3. $^{13}\text{C}\{^1\text{H}\}$ NMR spectrum of **1** in CDCl_3 at 101 MHz

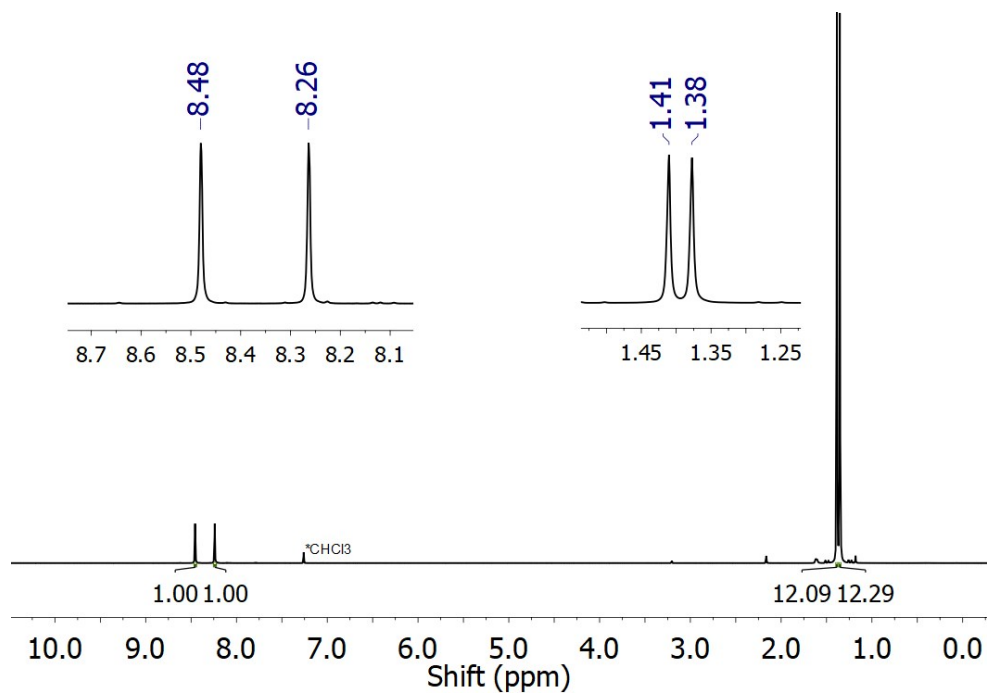


Figure S4. ^1H NMR spectrum of **2** in CDCl_3 at 500 MHz

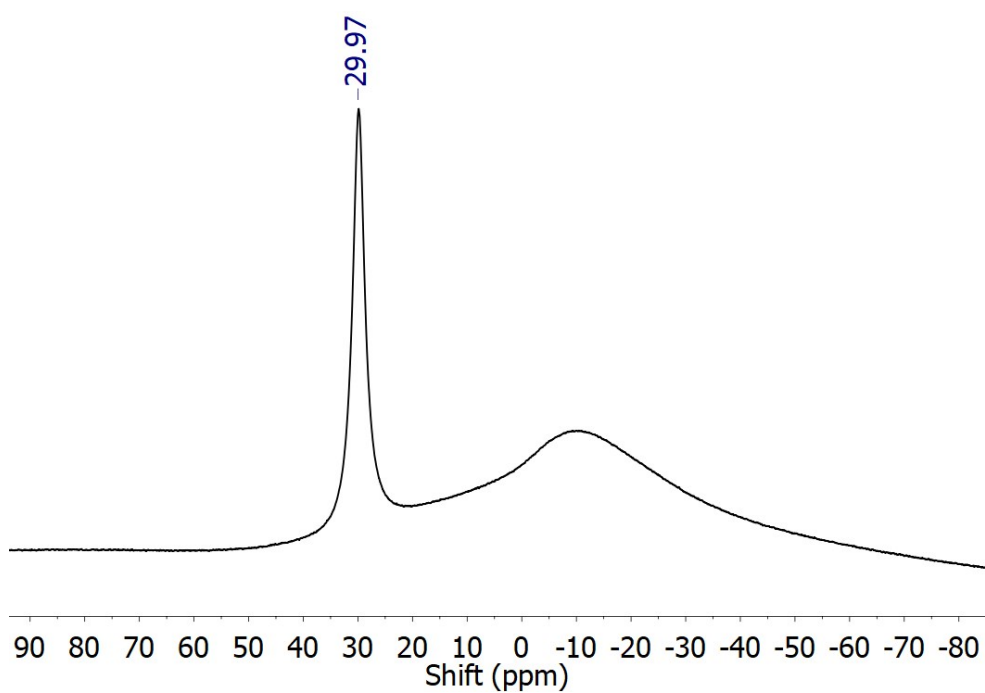


Figure S5. $^{11}\text{B}\{^1\text{H}\}$ NMR spectrum of **2** in CDCl_3 at 128 MHz

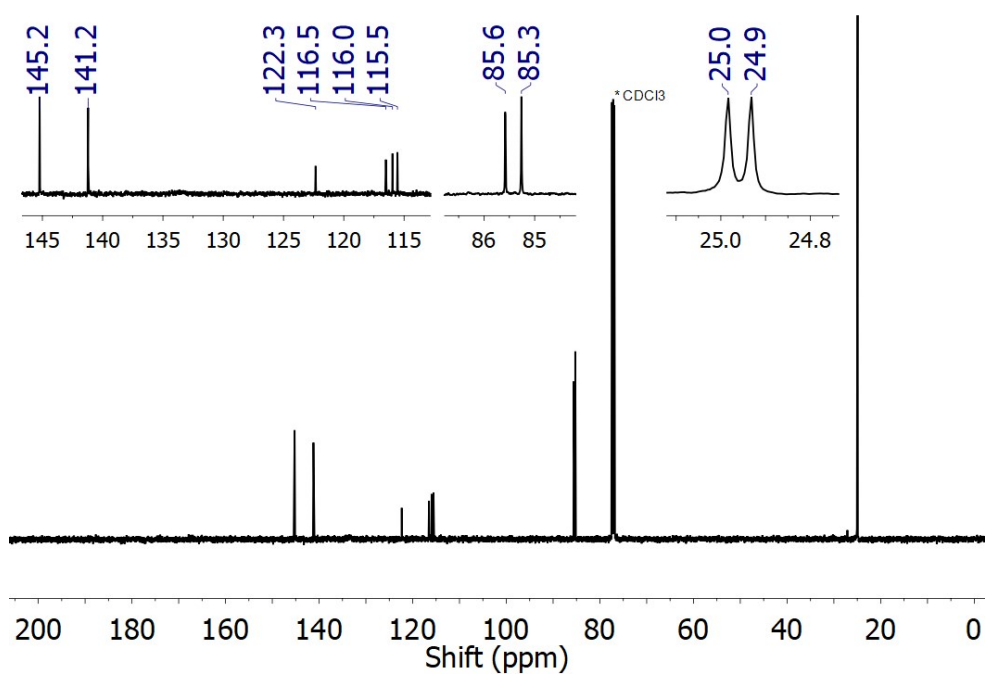


Figure S6. $^{13}\text{C}\{^1\text{H}\}$ NMR spectrum of **2** in CDCl_3 at 126 MHz

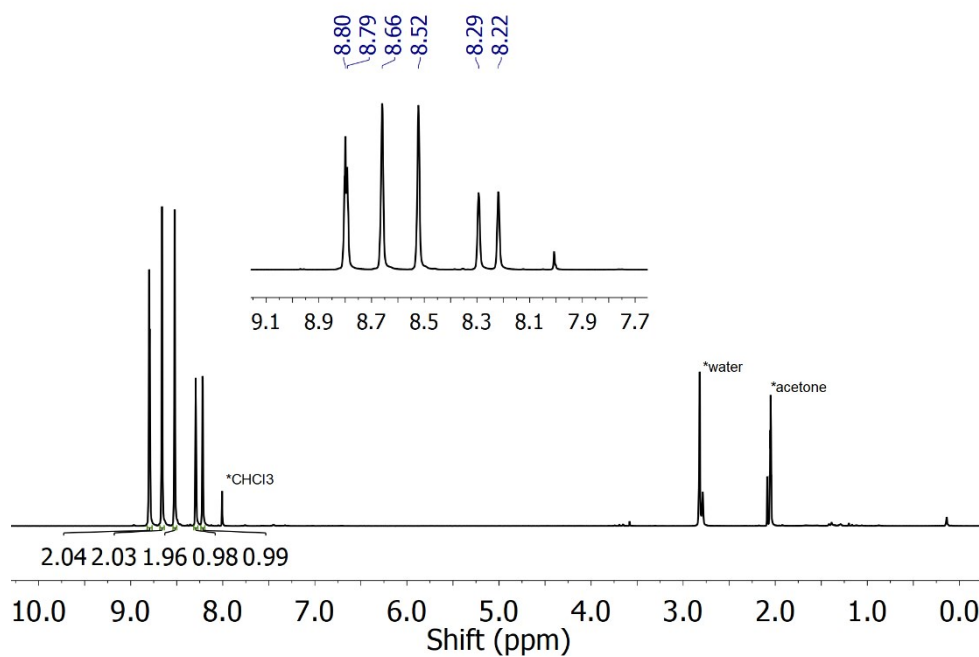


Figure S7. ¹H NMR spectrum of **3** in acetone-d₆ at 500 MHz

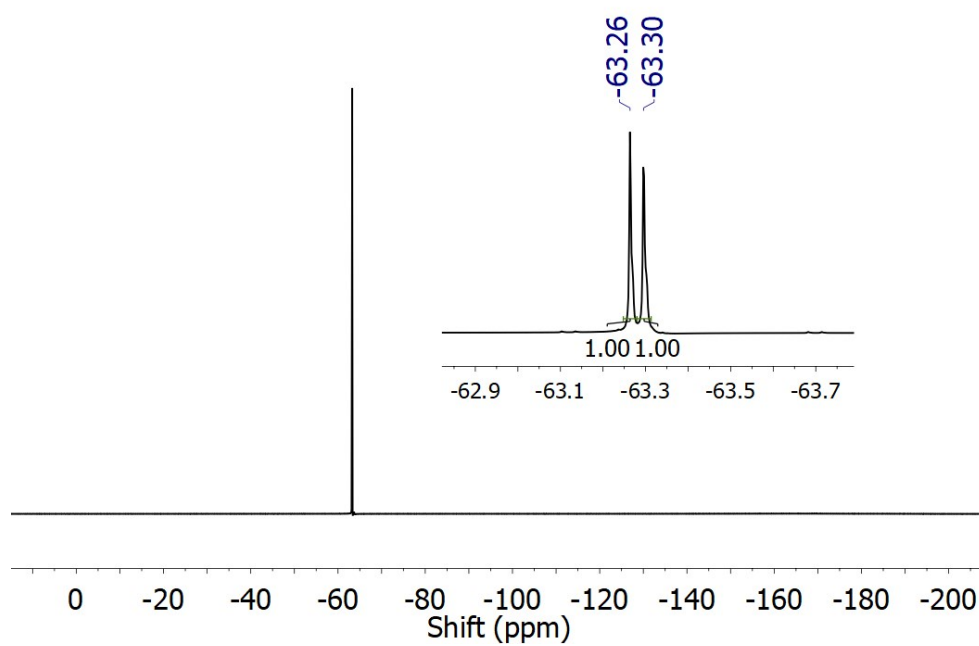


Figure S8. ¹⁹F NMR spectrum of **3** in acetone-d₆ at 470 MHz

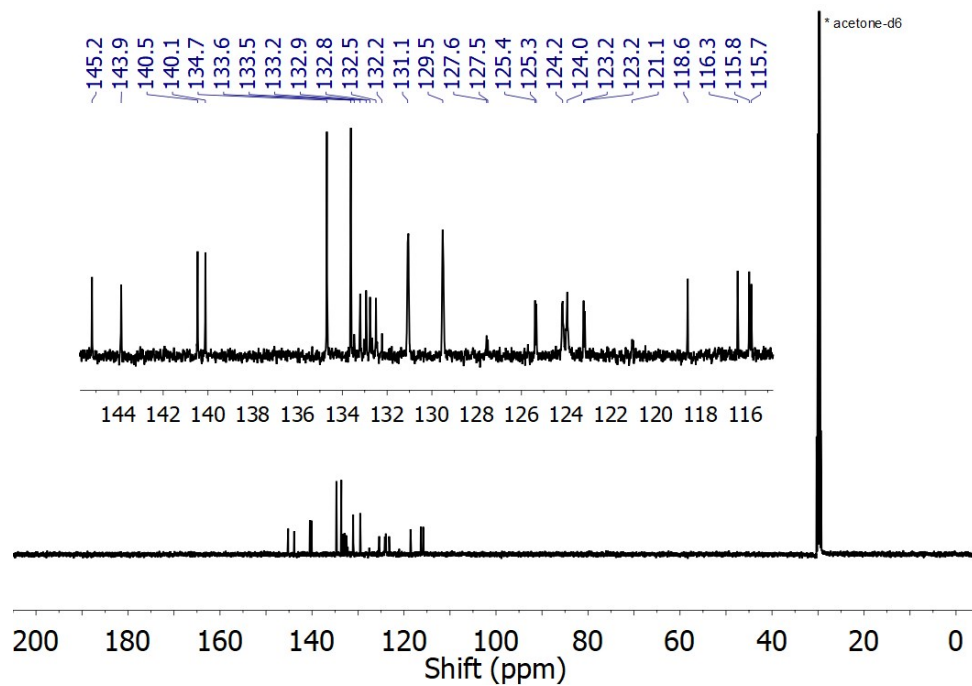


Figure S9. $^{13}\text{C}\{^1\text{H}\}$ NMR spectrum of **3** in acetone- d_6 at 126 MHz. Individual peaks of quartets labeled, while only the central peak of the septets and multiplets are labeled for clarity.

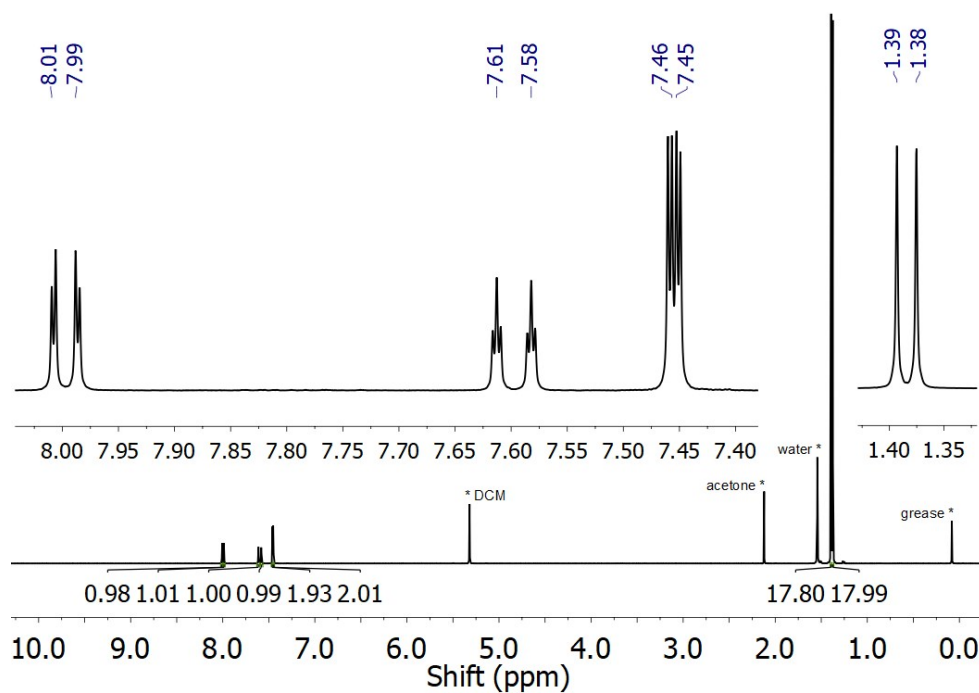


Figure S10. ^1H NMR spectrum of **4** in CD_2Cl_2 at 400 MHz

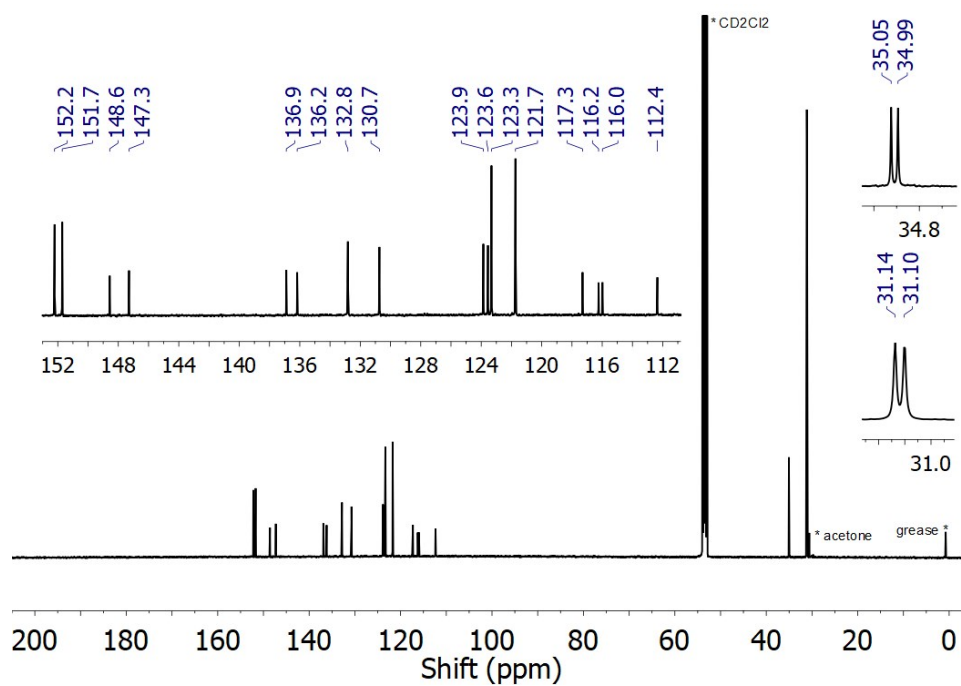


Figure S11. ¹³C{¹H} NMR spectrum of **4** in CD₂Cl₂ at 126 MHz

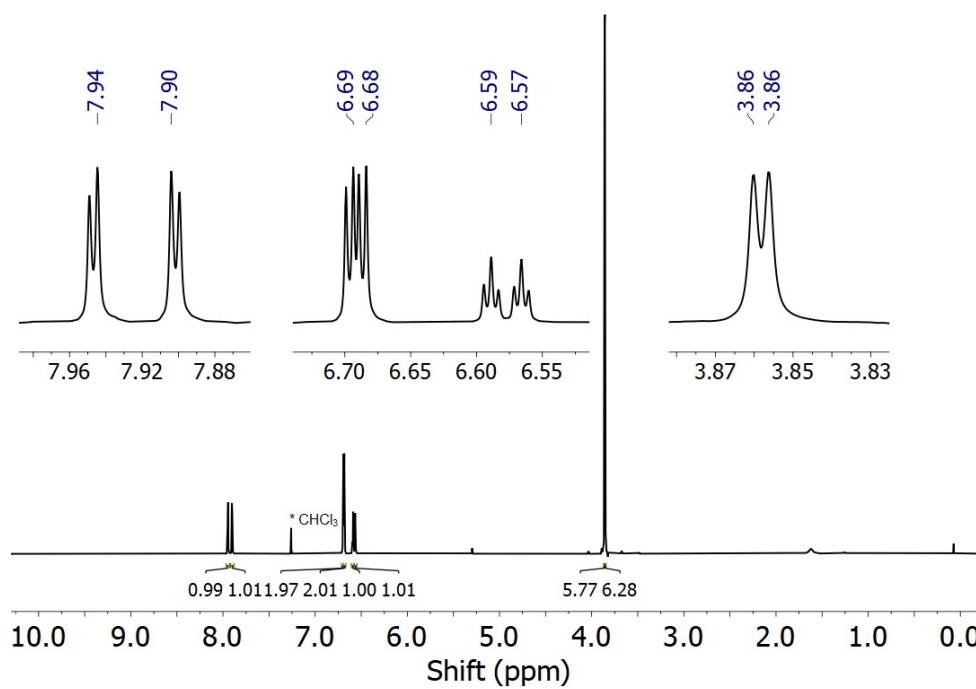


Figure S12. ¹H NMR spectrum of **5** in CDCl₃ at 400 MHz

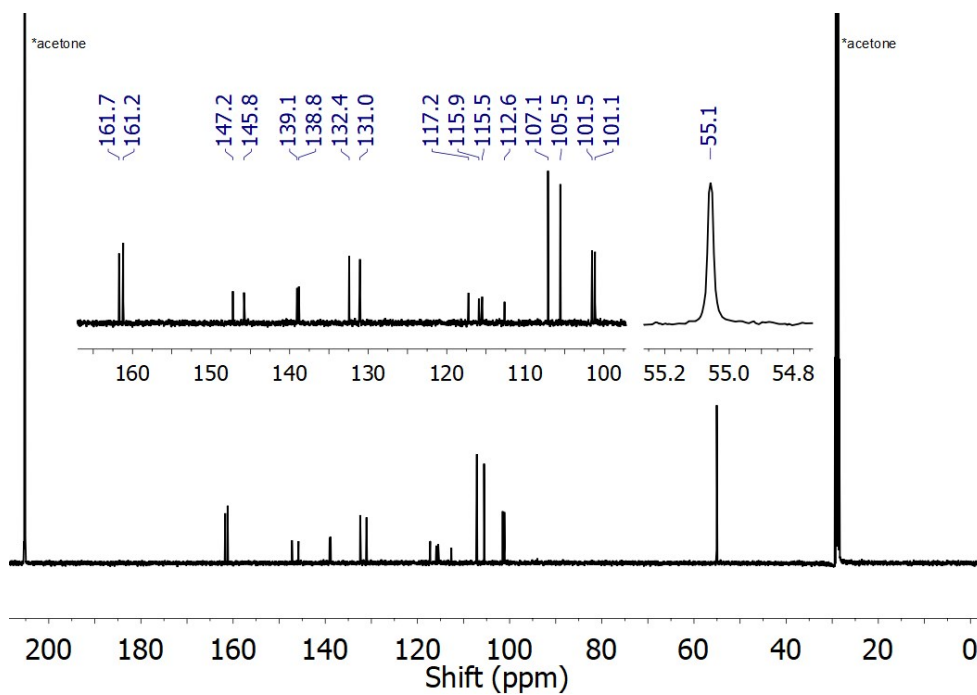


Figure S13. ¹³C{¹H} NMR spectrum of **5** in acetone-d₆ at 126 MHz

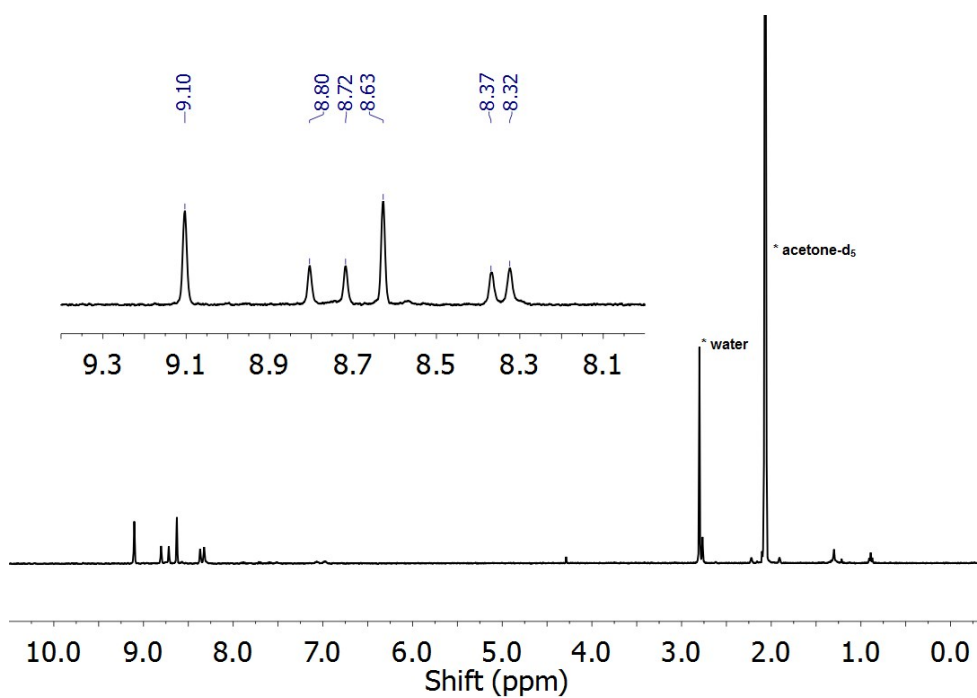


Figure S14. ¹H NMR spectrum of **6** in acetone-d₆ at 400 MHz

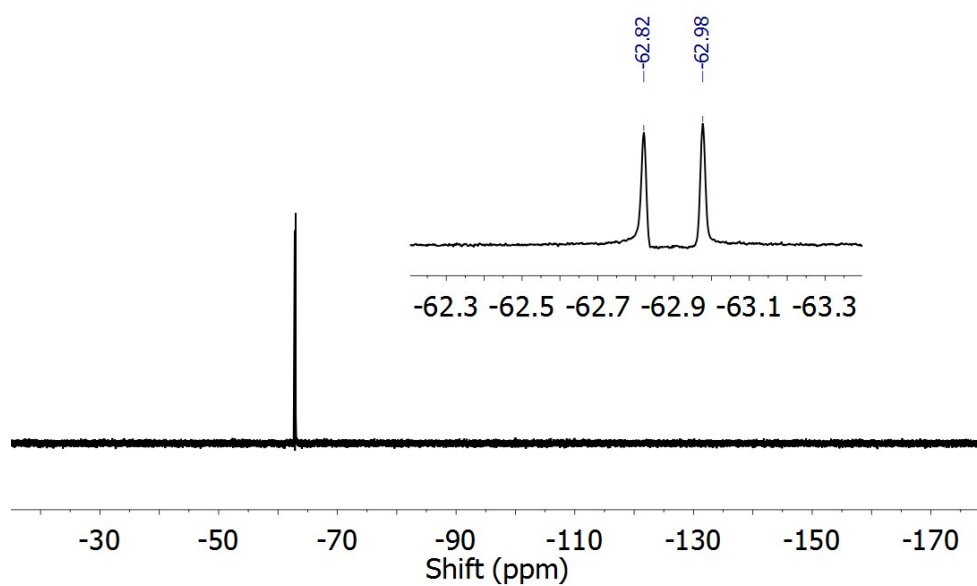


Figure S15. ^{19}F NMR spectrum of **6** in acetone- d_6 at 376 MHz

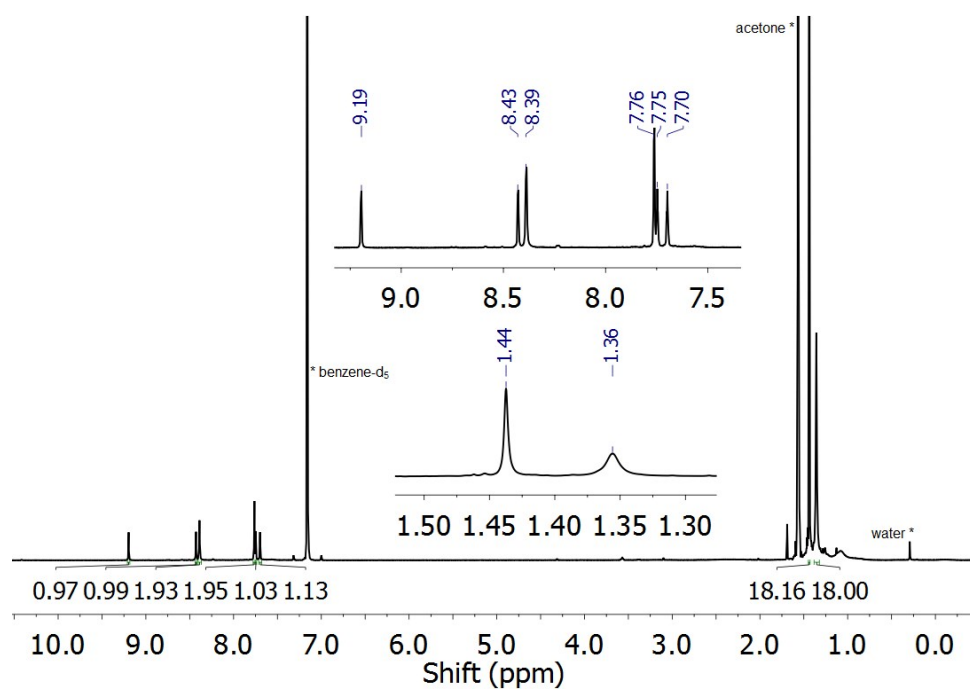


Figure S16. ^1H NMR spectrum of **7** in benzene- d_6 at 500 MHz

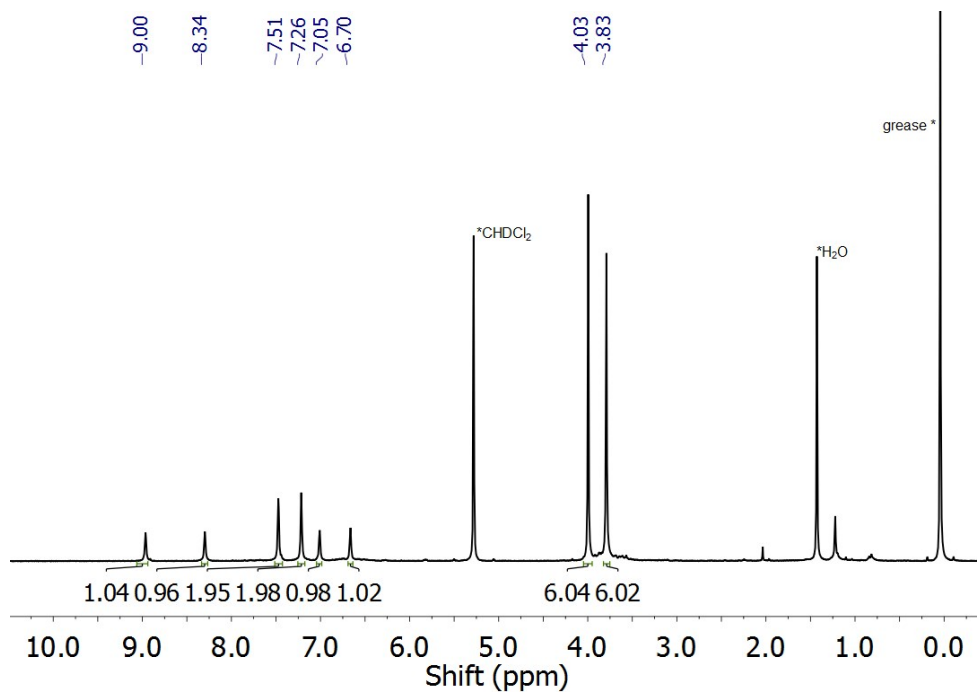


Figure S17. ¹H NMR spectrum of **8** in CD₂Cl₂ at 400 MHz

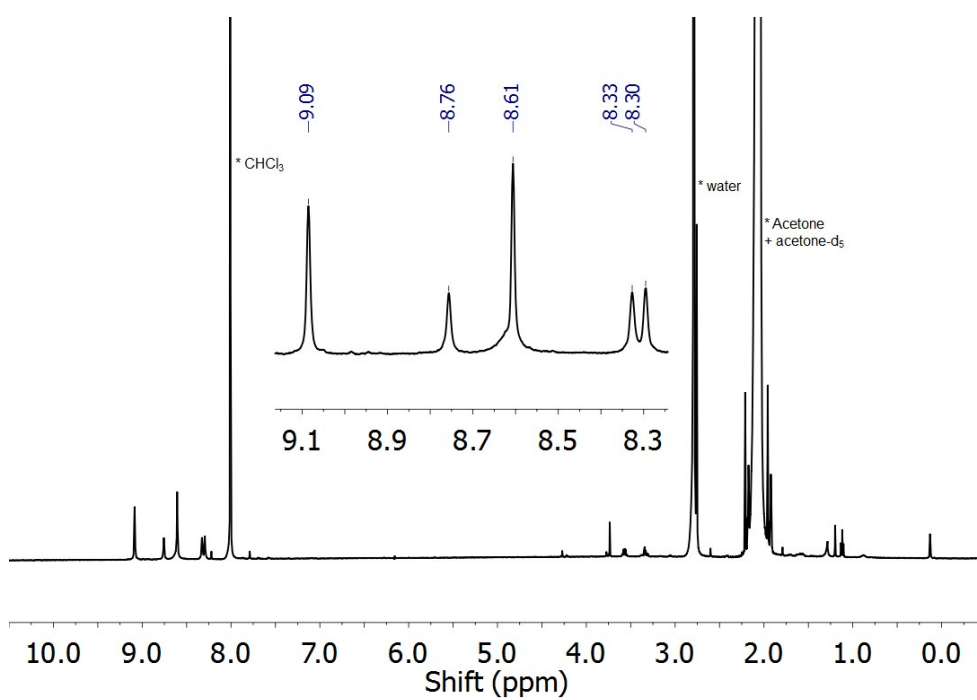


Figure S18. ¹H NMR spectrum of **9** in acetone-d₆ at 500 MHz

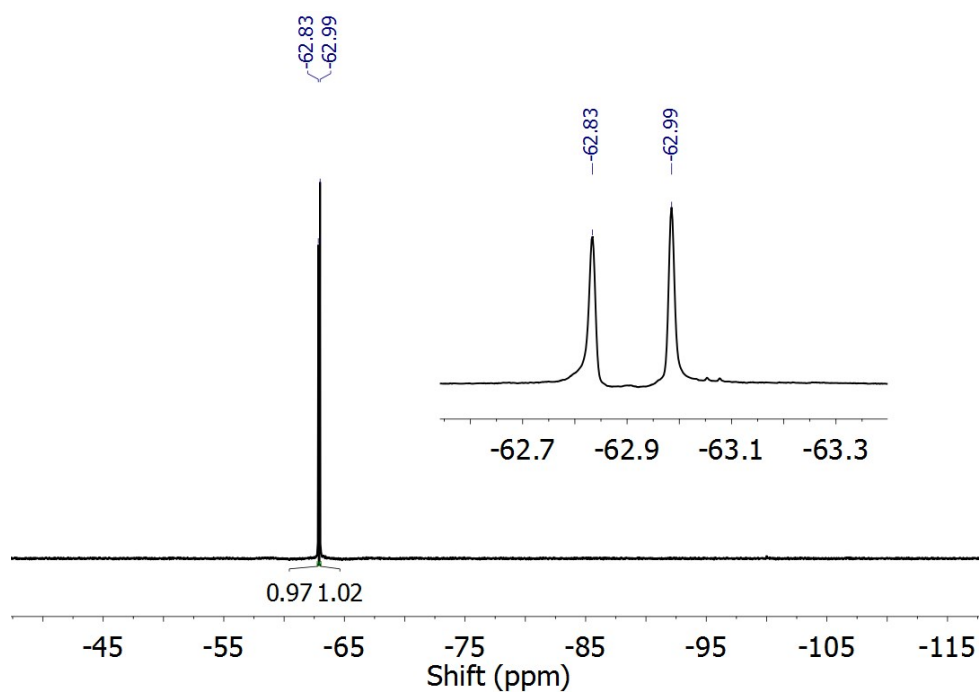


Figure S19. ^{19}F NMR spectrum of **9** in acetone- d_6 at 471 MHz

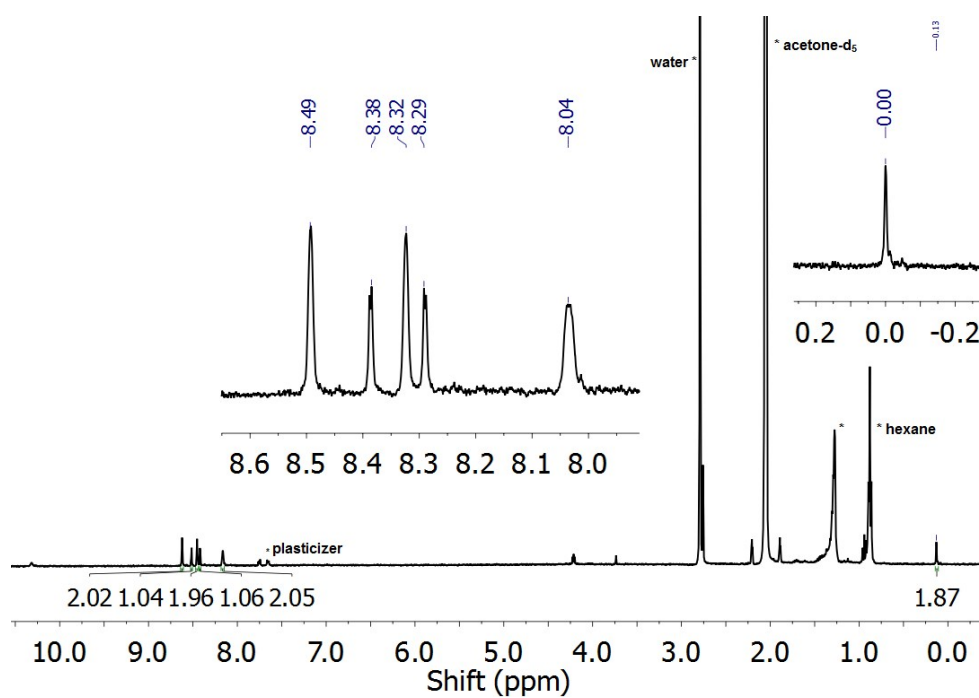


Figure S20. ^1H NMR spectrum of **10** in acetone- d_6 at 376 MHz. The signal at 0.0 ppm corresponds to the exchangeable inner N-H protons of the free-base phthalocyanine, which diminish upon a D_2O shake.

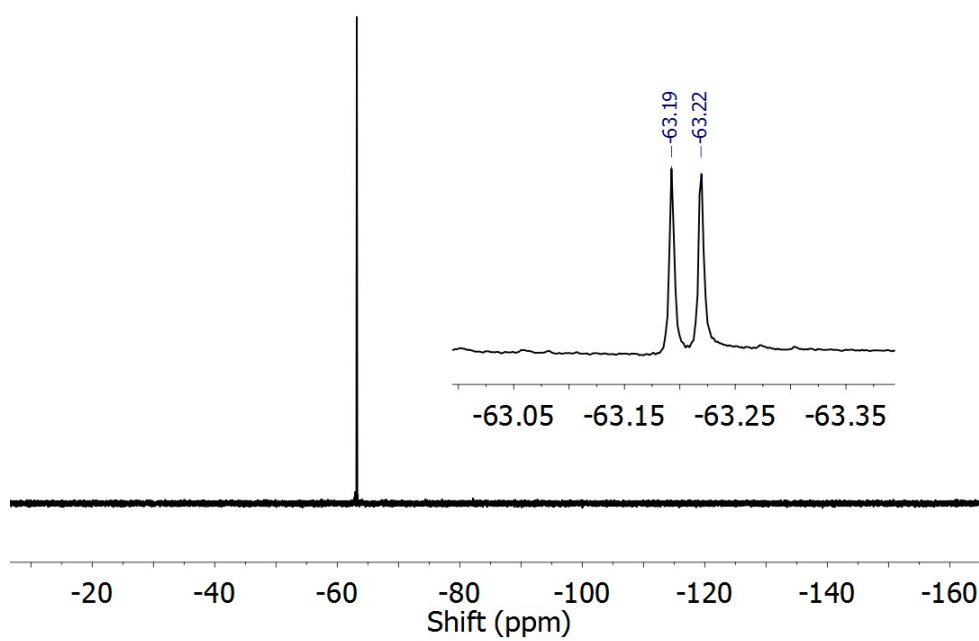


Figure S21. ^{19}F NMR spectrum of **10** in acetone- d_6 at 376 MHz

Single-Crystal X-ray Diffraction

Table S1. Crystal data and X-ray experimental details for compound **1-5**

Compound	1	2	3	4
CCDC	1989726	1989727	1989434	1989438
Formula	C ₁₄ H ₁₆ BN ₂ O _{2.25}	C ₂₀ H ₂₆ B ₂ N ₂ O ₄	C ₂₄ H ₈ F ₁₂ N ₂ , 0.5[C ₆ H ₁₄]	C ₃₆ H ₄₄ N ₂
<i>M</i> _r	259.10	380.05	595.41	504.73
Crystal size [mm ³]	0.39 × 0.36 × 0.16	0.34 × 0.24 × 0.17	0.29 × 0.23 × 0.20	0.21 × 0.16 × 0.15
Crystal system	Orthorhombic	Monoclinic	Monoclinic	Triclinic
Space group	<i>Pnma</i>	<i>P2₁/c</i>	<i>C2/c</i>	<i>P</i> $\bar{1}$
<i>T</i> /K	120	120	120	120
<i>a</i> [Å]	26.6432(10)	13.6361(9)	26.3200(12)	8.9530(12)
<i>b</i> [Å]	6.8628(5)	11.8505(8)	8.4133(4)	11.4420(14)
<i>c</i> [Å]	7.9989(3)	13.0118(8)	22.4036(10)	15.907(2)
α [°]	90	90	90	105.674(4)
β [°]	90	92.200(2)	95.7836(14)	90.147(4)
γ [°]	90	90	90	102.422(4)
<i>V</i> [Å ³]	1462.57(13)	2101.1(2)	4935.8(4)	1529.0(3)
<i>Z</i>	4	4	8	2
ρ_{calcd} [g cm ⁻³]	1.177	1.201	1.603	1.096
λ [Å]	0.71073	0.71073	0.71073	0.71073
μ [mm ⁻¹]	0.079	0.082	0.158	0.063
<i>F</i> (000)	548.0	808.0	2392.0	548.0
2 θ range [°]	5.318-49.998	4.556-52.00	4.554-53.588	4.668-51.994
	-30 ≤ <i>h</i> ≤ 31	-16 ≤ <i>h</i> ≤ 16	-32 ≤ <i>h</i> ≤ 33	-11 ≤ <i>h</i> ≤ 11
Index ranges	-8 ≤ <i>k</i> ≤ 8	-14 ≤ <i>k</i> ≤ 14	-10 ≤ <i>k</i> ≤ 10	-14 ≤ <i>k</i> ≤ 14
	-9 ≤ <i>l</i> ≤ 9	-15 ≤ <i>l</i> ≤ 16	-28 ≤ <i>l</i> ≤ 26	-19 ≤ <i>l</i> ≤ 19
Reflections collected	15027	54792	34315	29621
	1406	4131	5262	5988
Independent reflections	<i>R</i> _{int} = 0.0420	<i>R</i> _{int} = 0.0629	<i>R</i> _{int} = 0.0422	<i>R</i> _{int} = 0.1109
Refinement method	Full-matrix least-squares on <i>F</i> ²			
Data/restraints/parameters	1406/177/145	4131/6/279	5262/48/408	5988/0/355
Goodness of fit on <i>F</i> ²	1.052	1.067	1.033	1.008
Final <i>R</i> indices (<i>I</i> ≥ 2σ(<i>I</i>))	<i>R</i> ₁ = 0.0749 <i>wR</i> ₂ = 0.1924	<i>R</i> ₁ = 0.0450 <i>wR</i> ₂ = 0.0962	<i>R</i> ₁ = 0.0474 <i>wR</i> ₂ = 0.1128	<i>R</i> ₁ = 0.0622 <i>wR</i> ₂ = 0.1185
Final <i>R</i> indices (all data)	<i>R</i> ₁ = 0.0968 <i>wR</i> ₂ = 0.2123	<i>R</i> ₁ = 0.0627 <i>wR</i> ₂ = 0.1042	<i>R</i> ₁ = 0.0626 <i>wR</i> ₂ = 0.1225	<i>R</i> ₁ = 0.1265 <i>wR</i> ₂ = 0.1418
Largest difference peak/hole [e Å ⁻³]	0.51/-0.42	0.24/-0.20	0.45/-0.39	0.40/-0.24

Table S2. Crystal data and X-ray experimental details for compound **5**, **6**, **7** and **9**

Compound	5	6	7*	9*
CCDC	1989433	1989435	1989436	1989437
Formula	C ₂₄ H ₂₀ N ₂ O ₄	C ₉₉ H ₃₅ F ₄₈ N _{8.6} O _{0.5} Zn, 6(C ₅ H ₅ N)	C ₁₄₄ N ₈ Zn, C ₁₄₄ N ₈ OZn, 8[H ₂ O], 16[C ₃ H ₆ O]	C ₉₆ H ₃₄ F ₄₈ MgN ₈ O, 2.5[C ₃ H ₆ O], 2.5[C ₆ H ₁₄]
<i>M_r</i>	400.44	2804.72	3829.78	2612.24
Crystal size [mm ³]	0.36 × 0.29 × 0.15	0.37 × 0.35 × 0.19	0.24 × 0.22 × 0.14	0.25 × 0.12 × 0.01
Crystal system	Triclinic	Triclinic	Triclinic	Triclinic
Space group	<i>P</i> $\bar{1}$	<i>P</i> $\bar{1}$	<i>P</i> $\bar{1}$	<i>P</i> $\bar{1}$
<i>T</i> /K	120	120	120	150
<i>a</i> [Å]	7.6587(6)	9.8387(6)	19.5182(8)	9.3959(12)
<i>b</i> [Å]	11.0602(8)	15.9659(11)	19.5876(9)	15.9579(18)
<i>c</i> [Å]	12.3929(8)	19.7070(13)	22.5521(9)	19.8503(14)
α [°]	87.763(5)	104.0668(18)	99.467(3)	104.367(8)
β [°]	74.272(6)	102.2170(17)	111.596(2)	101.254(8)
γ [°]	87.728(6)	94.6532(19)	95.906(2)	97.571(10)
<i>V</i> [Å ³]	1009.23(13)	2906.0(3)	7781.0(6)	2776.5(5)
<i>Z</i>	2	1	1	1
ρ_{calcd} [g cm ⁻³]	1.3176	1.603	—	1.562
λ [Å]	0.71073	0.71073	1.54178	1.54184
μ [mm ⁻¹]	0.091	0.350	0.537	1.393
<i>F</i> (000)	420.2	1407.0	1908.0	1442.0
2 θ range [°]	4.96–52.00	3.87–51.996	4.318–152.208	9.468–108.624
Index ranges	–10 ≤ <i>h</i> ≤ 10	–12 ≤ <i>h</i> ≤ 11	–23 ≤ <i>h</i> ≤ 20	–6 ≤ <i>h</i> ≤ 9
	–14 ≤ <i>k</i> ≤ 14	–19 ≤ <i>k</i> ≤ 19	–24 ≤ <i>k</i> ≤ 24	–16 ≤ <i>k</i> ≤ 16
	–16 ≤ <i>l</i> ≤ 16	–24 ≤ <i>l</i> ≤ 24	–28 ≤ <i>l</i> ≤ 28	–20 ≤ <i>l</i> ≤ 16
Reflections collected	11573	83083	101564	10196
Independent reflections	3968	11412	31289	6083
	<i>R</i> _{int} = 0.0553	<i>R</i> _{int} = 0.1095	<i>R</i> _{int} = 0.2699	<i>R</i> _{int} = 0.0646
Refinement method	Full-matrix least-squares on <i>F</i> ²			
Data/restraints/parameters	3968/0/275	11412/240/1072	31289/6/1393	6083/389/867
Goodness of fit on <i>F</i> ²	1.049	1.018	1.008	0.962
Final <i>R</i> indices (<i>I</i> ≥ 2 σ (<i>I</i>))	<i>R</i> ₁ = 0.0523	<i>R</i> ₁ = 0.0718	<i>R</i> ₁ = 0.1535	<i>R</i> ₁ = 0.0852
	<i>wR</i> ₂ = 0.1004	<i>wR</i> ₂ = 0.1728	<i>wR</i> ₂ = 0.3901	<i>wR</i> ₂ = 0.2260
Final <i>R</i> indices (all data)	<i>R</i> ₁ = 0.0909	<i>R</i> ₁ = 0.1163	<i>R</i> ₁ = 0.2974	<i>R</i> ₁ = 0.1428
	<i>wR</i> ₂ = 0.1194	<i>wR</i> ₂ = 0.2016	<i>wR</i> ₂ = 0.4740	<i>wR</i> ₂ = 0.2732
Largest difference peak/hole [e Å ⁻³]	0.42/–0.40	0.77/–0.59	0.55/–0.57	0.84/–0.33

* Although the crystal structures obtained were of relatively low quality, due to extensive disorder of the many substituents and of the significant quantity of highly disordered solvent molecules incorporated in the structures, they do confirm the nominal *C*_{4h} symmetry conclusively.

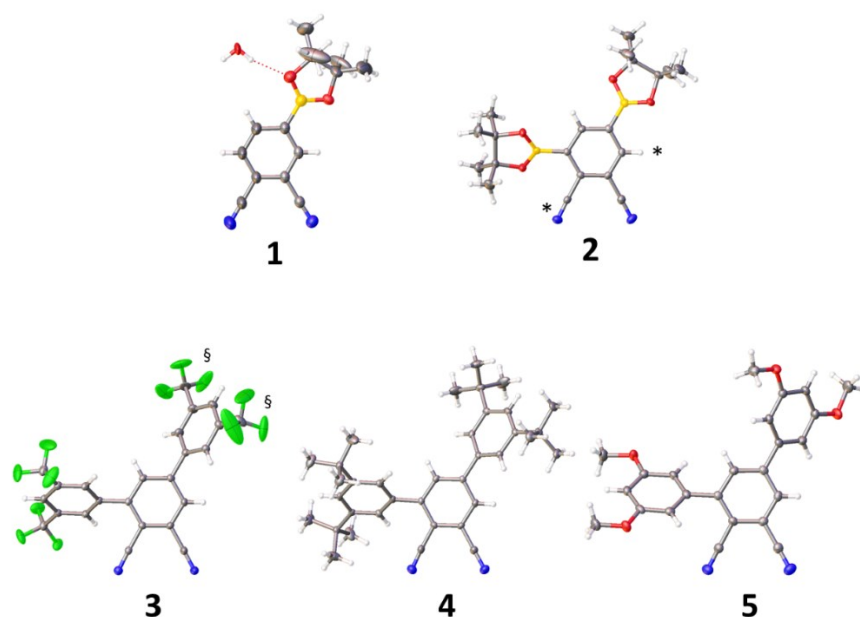


Figure S22. Molecular structures of **1-5** obtained by SC-XRD. The occupancy of the H₂O molecule in the structure of **1** is 0.25. For **2**, only the major (94%) orientation is shown. Crystallographic positional disorder gives a second minor (6%) component in which the cyano group and H atom marked * are switched in the structure; these molecules are chemically equivalent. For **3**, the two CF₃ groups marked § have been modelled as rotationally disordered over two sites; only the major (67% and 50%) positions for each are shown, and residual solvent has been removed for clarity.

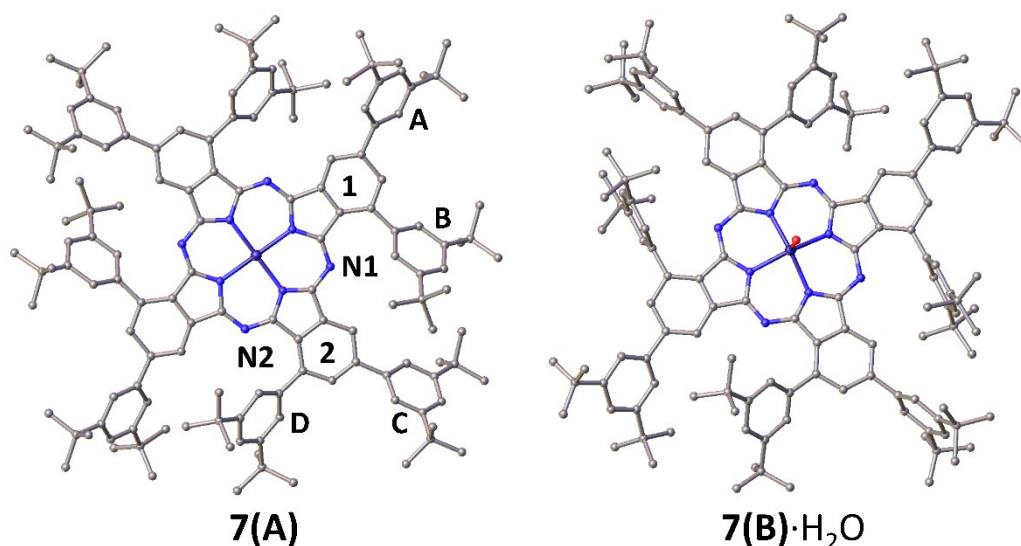


Figure S23. Molecular structures of **7** obtained by SC-XRD. The structure comprises two independent Pcs: potentially uncoordinated **7(A)** and **7(B)·H₂O**. Disordered solvent molecules have been removed for clarity. Note that the Zn atom of **7(A)** may also be ligated, but the ligand could not be identified from the Fourier map.

Absorption and Emission Spectra

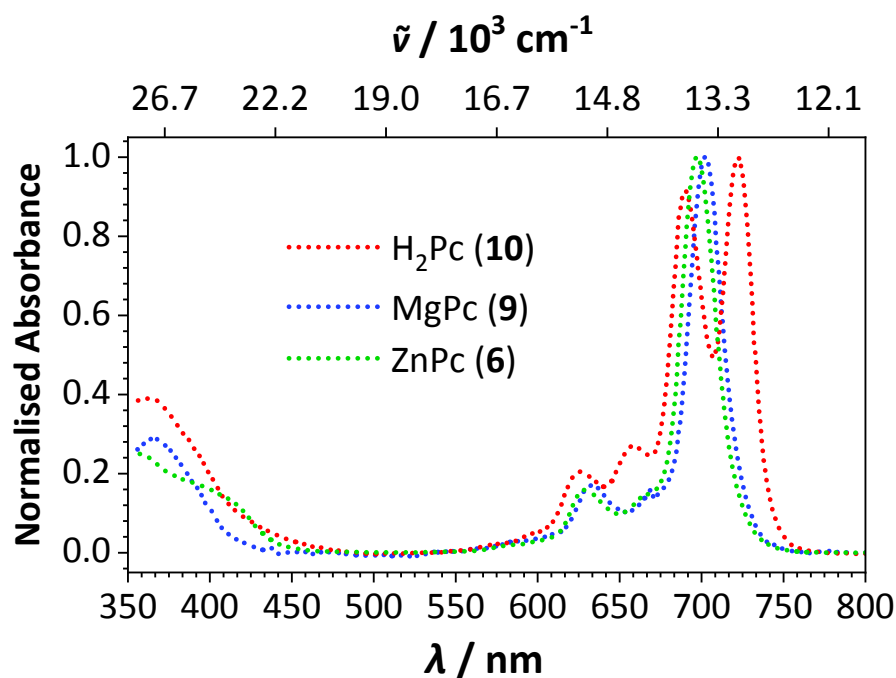


Figure S24. A comparison of the absorption spectra of **6**, **9** and **10** in CH₂Cl₂ solution

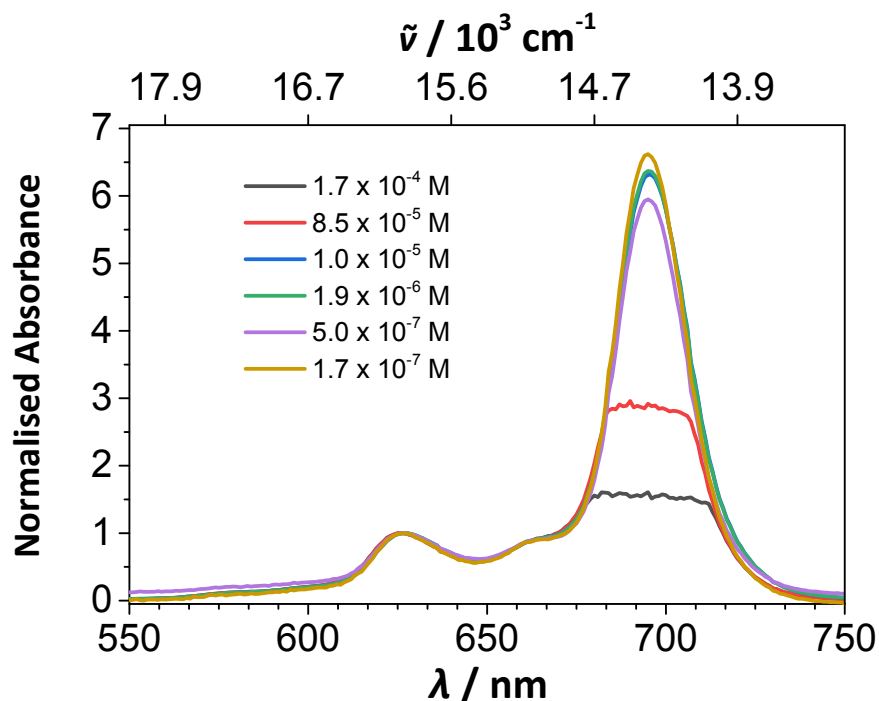


Figure S25. A comparison of the Q band region of the UV-visible absorption spectra of **6** as a function of concentration in acetone solution. At high concentrations the Q₀₀ absorbance was outside of the dynamic range of the spectrometer; however, the lack of broadening and independence of the Q₀₂ band on concentration indicate that **6** does not aggregate at the concentrations listed in the legend. Spectra were normalized at the Q₀₂ peak (627 nm).

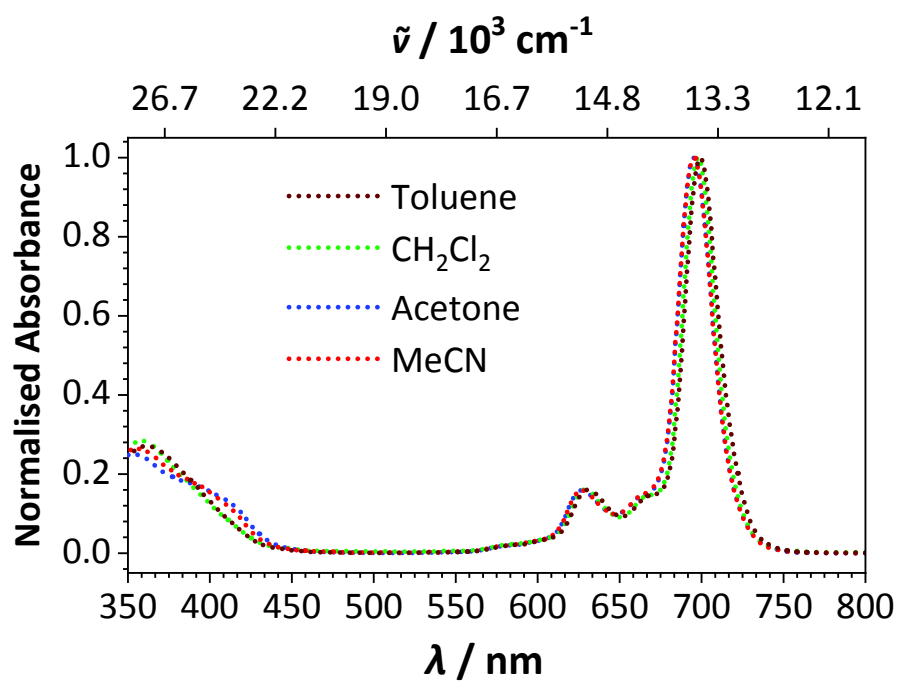


Figure S26. Absorption spectra of **6** in solvents of different polarity, as indicated in the legend

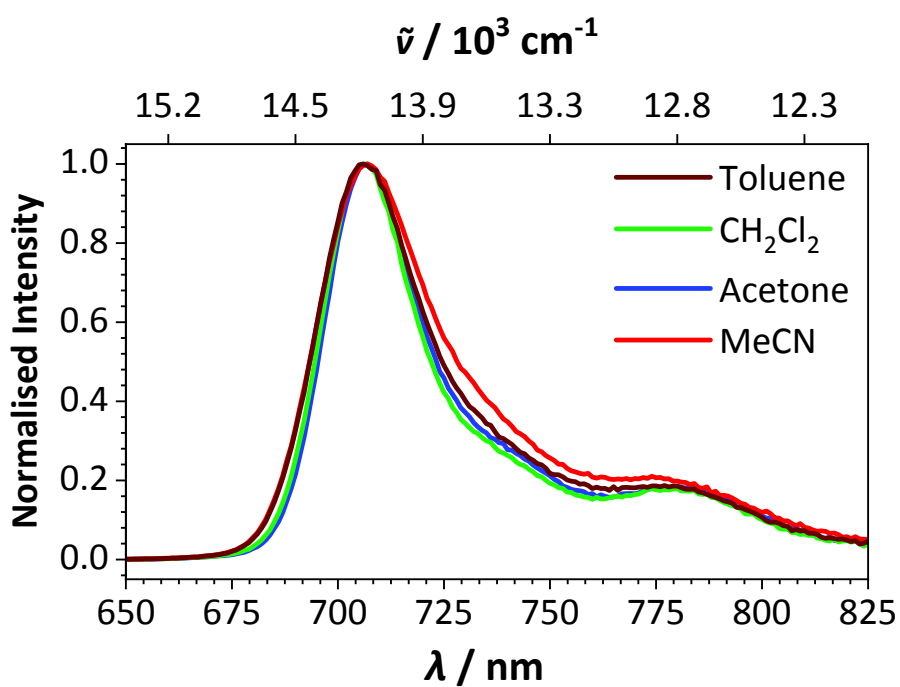


Figure S27. Emission spectra of **6** in solvents of different polarity, as indicated in the legend

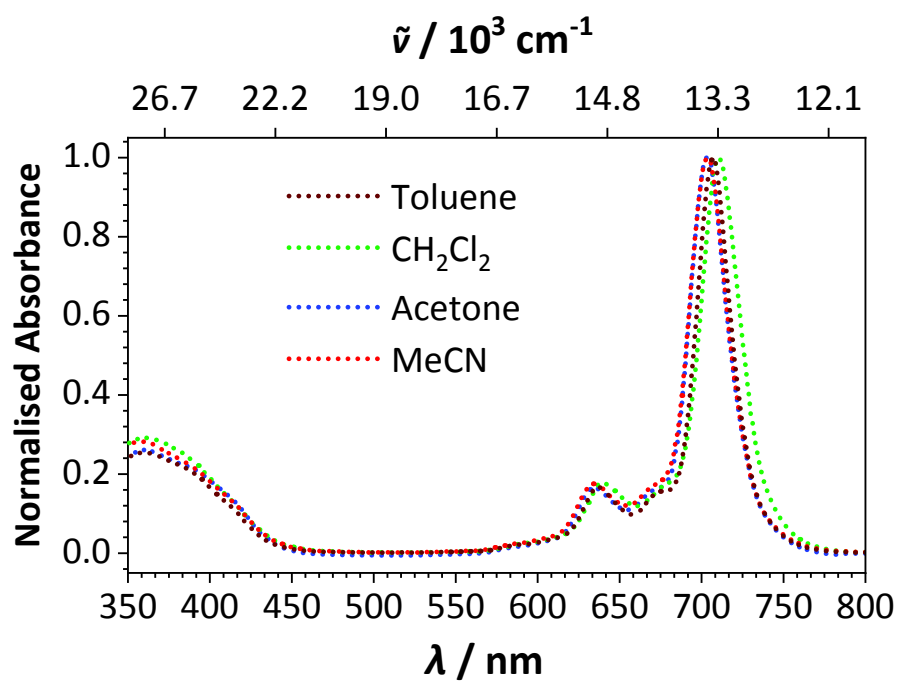


Figure S28. Absorption spectra of **7** in solvents of different polarity, as indicated in the legend

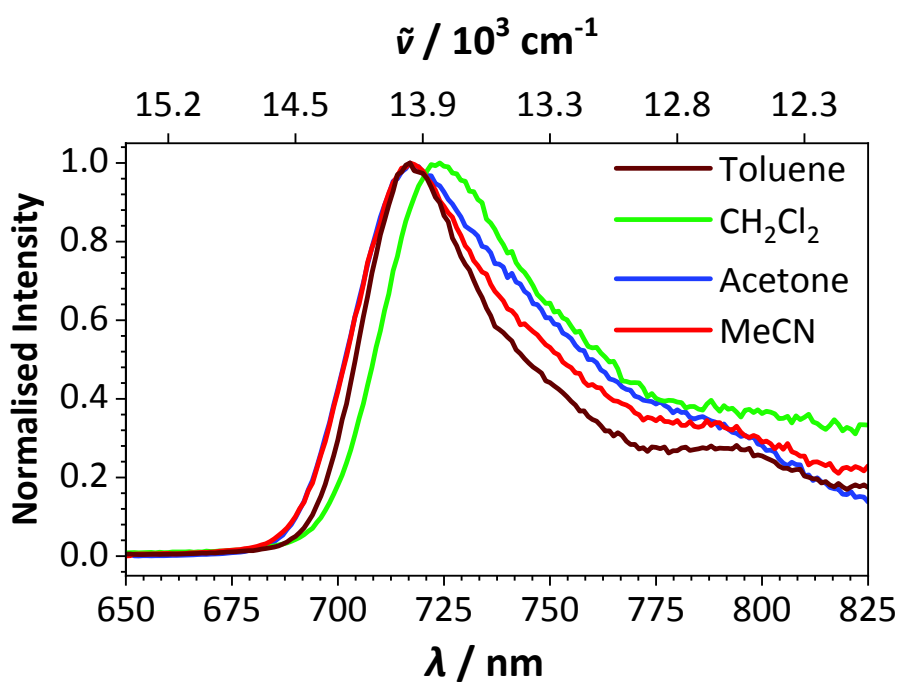


Figure S29. Emission spectra of **7** in solvents of different polarity, as indicated in the legend

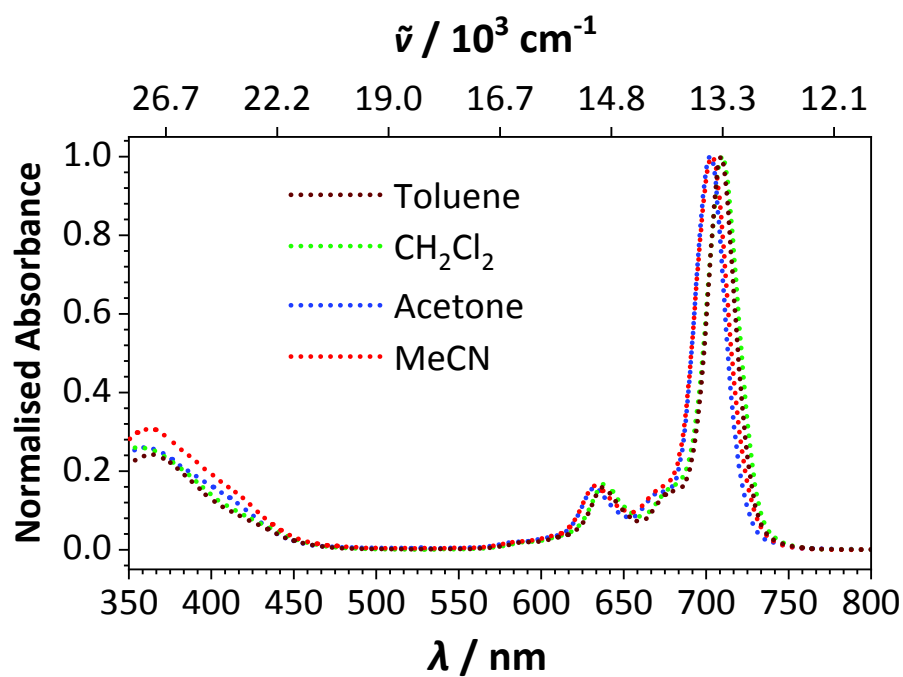


Figure S30. Absorption spectra of **8** in solvents of different polarity, as indicated in the legend

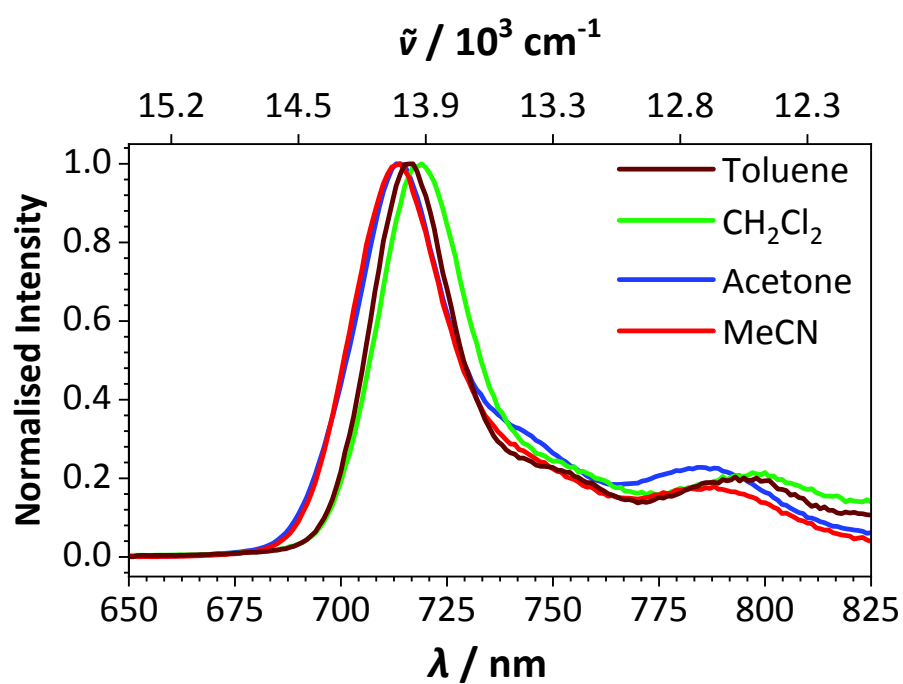


Figure S31. Emission spectra of **8** in solvents of different polarity, as indicated in the legend

References

1. R. Uson, L. A. Oro, J. A. Cabeza, H. E. Bryndza, M. P. Stepro, *Inorg. Synth.*, 1985, **23**, 126-129.
2. O. V. Dolomanov, L. J. Bourhis, R. J. Gildea, J. A. K. Howard, H. Puschmann, *J. Appl. Crystallogr.*, 2009, **42**, 339-341.
3. A. C. Beveridge, B. A. Bench, S. A. Gorun, G. J. Diebold, *J. Phys. Chem. A*, 2003, **107**, 5138-5143.
4. W. Spiller, H. Kliesch, D. Wöhrle, S. Hackbarth, B. Röder, G. Schnurpfeil, *J. Porphyr. Phthalocyanines*, 1998, **2**, 145-158.